

# Magnetic susceptibility of the normal–superconducting transition in high-purity single crystal $\alpha$ -uranium

J. L. O'Brien,<sup>1,2\*</sup> A. R. Hamilton,<sup>2</sup> R. G. Clark,<sup>2</sup> C. H. Mielke,<sup>3</sup> J. L. Smith,<sup>3</sup> J. C. Cooley,<sup>3</sup> D. G. Rickel,<sup>3</sup> R. P. Starrett,<sup>2</sup> D. J. Reilly,<sup>2</sup> N. E. Lumpkin,<sup>2</sup> R. J. Hanrahan, Jr.,<sup>3</sup> and W. L. Hults<sup>3</sup>

<sup>1</sup>Centre for Quantum Computer Technology, Department of Physics, University of Queensland, Brisbane 4072, Australia

<sup>2</sup>Centre for Quantum Computer Technology, School of Physics, University of New South Wales, Sydney 2052, Australia

<sup>3</sup>Los Alamos National Laboratory, Los Alamos, NM 87545, USA

(October 24, 2018)

We report the first complex ac magnetic susceptibility measurements of a superconducting transition in very high quality single crystal  $\alpha$ -uranium using micro-fabricated coplanar magnetometers. We identify an onset of superconductivity at  $T \approx 0.7$  K in both the real and imaginary components of the susceptibility which is confirmed by resistivity data. A superconducting volume fraction argument, based on a comparison with a calibration  $\text{YBa}_2\text{Cu}_3\text{O}_{7-\delta}$  sample, indicates that superconductivity in these samples may be filamentary. Our data also demonstrate the sensitivity of the coplanar micro-magnetometers, which are ideally suited to measurements in pulsed magnetic fields exceeding 100 T.

74.70.Ad, 74.60.-w, 74.25.Ha, 07.55.Jg

Since the 1942 discovery of superconductivity in uranium a coherent picture of the phenomenon in its compounds has been developed, perturbed only by the identification of heavy fermion superconductors amongst these materials.<sup>1</sup> The nature of superconductivity in elemental uranium, however, has remained enigmatic, largely due to the difficulty in producing pure single crystal samples. In its room temperature  $\alpha$ -phase, uranium is not a normal bulk superconductor: it shows a reverse isotope effect, with transition temperatures increasing with mass squared;<sup>2</sup> and competes with the formation of charge density wave (CDW) states with transitions at 43, 37 and 23 K.<sup>3,4</sup> As the heaviest naturally occurring element uranium exhibits a CDW state (typically observed in quasi-one-dimensional materials), is one of very few elemental type II superconductors, has a crystal structure which is unique at ambient pressures,<sup>1</sup> and has a valence shell configuration which breaks Hund's third rule.<sup>5</sup>

Early magnetic measurements of  $\alpha$ -uranium showed superconductivity with critical temperatures ( $T_c$ 's) ranging from 0.68–1.3 K for polycrystalline samples.<sup>1</sup> In contrast, an upper limit of  $T_c = 0.1$  K was observed for single crystals.<sup>6</sup> From these data  $T_c$  was understood to decrease with increasing sample purity.<sup>1</sup> The absence of a superconducting signature in corresponding specific heat measurements<sup>7,8</sup> led to the suggestion of “filamentary” as opposed to bulk superconductivity, where only regions of interconnected filaments exhibit superconductivity<sup>1,6–10</sup> (not to be confused with the use of filamentary in the early terminology of Type II materials to describe the mixed state). Pressure studies revealed  $\alpha$ -uranium to be one of the most strongly pressure enhanced superconductors, with a  $T_c$  rising to 2.3 K at  $P \approx 1$  GPa.<sup>10,11</sup> Specific-heat measurements at these pressures also revealed a bulk, rather than filamentary, superconducting state.<sup>8</sup> Following these experiments it was suggested that at  $P=0$  strain filaments are produced by the highly anisotropic thermal expansion of  $\alpha$ -uranium at low  $T$ .

Stabilized  $\gamma$ -U-X alloys ( $X = \text{Pt, Rh, Cr, Mo}$ ) also demonstrated bulk superconductivity, leading to the proposal of an alternative mechanism in which the filaments consist of impurity stabilized networks of  $\beta$ - and  $\gamma$ -phases of uranium.<sup>1,9</sup> There were even references to unpublished transmission electron microscopy images of the filaments.<sup>10</sup> Subsequent calorimetric studies indicated that  $\alpha$ -uranium was in fact a bulk superconductor at  $P=0$ .<sup>12</sup> It has since been accepted that superconductivity in  $\alpha$ -uranium is a bulk effect, although these results have never been reconciled with the earlier studies.<sup>1,6</sup> Very recent measurements on high-purity single crystals are also supportive of a bulk effect.<sup>13</sup> Despite the early intense efforts a complete picture of the superconducting state in this unusual material has yet to emerge.

In this communication we present the first complex ac magnetic susceptibility measurements on single crystal  $\alpha$ -uranium, of the highest purity yet produced.<sup>14</sup> An onset to a superconducting state at  $T \approx 0.7$  K is observed, confirmed by a transition to zero resistivity at  $T \approx 0.8$  K. We also find evidence for filamentary superconductivity based on a volume fraction comparison with measurements of a calibration sample of  $\text{YBa}_2\text{Cu}_3\text{O}_{7-\delta}$  (YBCO) that show a clear signature of the normal–superconducting transition at  $T \approx 95$  K. The results also suggest that  $T_c$  increases with sample purity, contrary to the earlier body of work, although the details of any filamentary nature may be important. The coplanar micro-magnetometers used in this work were specifically developed for high sensitivity magnetic measurements at low  $T$ . We identify the compatibility of these devices with the extreme environments of  $\mu$ s pulsed fields exceeding 100 T.<sup>15–18</sup>

Although zero resistivity is a classic signature of superconductivity, such measurements cannot distinguish between bulk and filamentary states because zero resistance is measured whenever there is a superconducting percolation path. In contrast, magnetic measurements

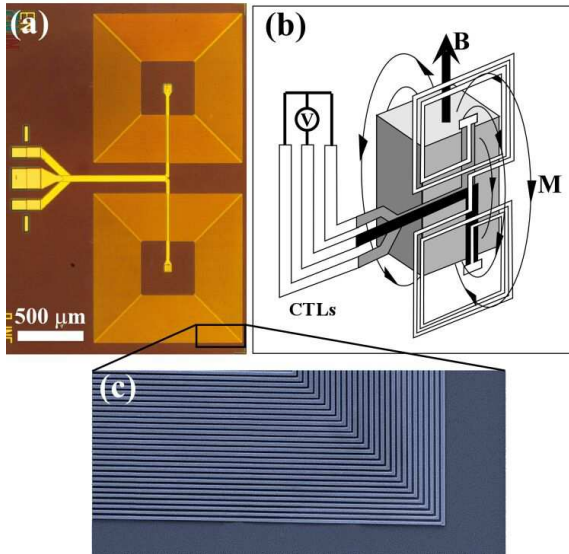


FIG. 1. Gold coplanar micro-magnetometer and sample mounting arrangement. (a) Micrograph of 120 turn magnetometer coils (b) schematic of mounting arrangement of the sample on the micro-magnetometer coils, showing how the induced magnetization generates a voltage  $V$ . (c) Scanning electron microscope image of the region indicated in (a)

have historically provided a very useful probe of superconductivity. In particular magnetic susceptibility measurements provide information about flux shielding and can offer insight into the superconducting volume fraction in non-bulk samples.<sup>19</sup> The development of sensitive magnetometers has enabled susceptibility measurements to be made where effects are slight and on small samples where signals are weak. Very sensitive superconducting quantum interference device (SQUID) magnetometers have been produced,<sup>20</sup> but are incapable of operating in high magnetic fields. Even more sensitive measurements have been made with cantilever magnetometers,<sup>21</sup> which are best suited to anisotropic samples, and there is evidence that they can be used in pulsed magnetic fields with sufficiently small samples.<sup>22</sup> Lithographically defined coplanar micro-magnetometers offer high sensitivity, near perfect compensation of the coils, the possibility of fabricating the coils directly onto a sample, and the ability to make measurements in high magnetic fields.

We have designed and micro-fabricated balanced, coplanar coil magnetometers specifically for magnetic measurements at low  $T$  and high  $B$ . Figure 1(a) shows an optical micrograph of a magnetometer fabricated on an insulating GaAs substrate using standard optical lithography techniques. It consists of two counter-wound coils with a center to center separation of 2mm. The coils are nearly perfectly compensated because of the precision of the lithography (Fig. 1c). The magnetometers have been designed to work with coplanar transmission

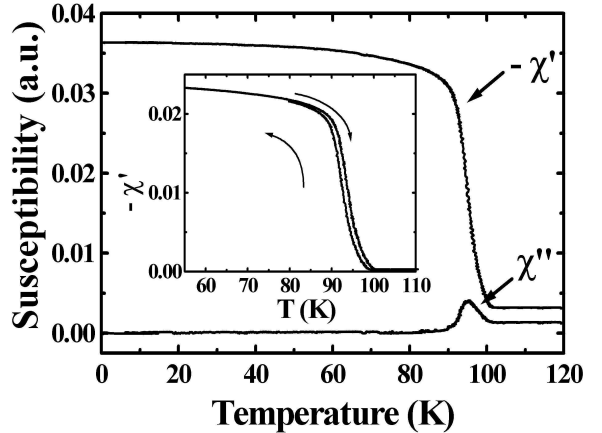


FIG. 2. Susceptibility vs. temperature for the YBCO sample. Both  $-\chi'$  and  $\chi''$  are shown for  $|B_{ac}|=35$  mT and  $\nu=150$  Hz. The inset shows a magnified view of the transition for up and down temperature sweeps revealing some hysteresis

lines (CTLs) on a printed circuit board, optimised for ultra-high magnetic field transport measurements<sup>15–17</sup> [illustrated schematically in Fig. 1(b)]. The two outer transmission lines are common and connect to the inner contact of the upper coil, while the center transmission line contacts the inner end of the lower coil. This multi-layer design uses insulating SiN layers to isolate the gold metal interconnects to the coils, and as a capping layer.

A liquid nitrogen cooled solenoid was used to apply a harmonic magnetic field  $B_{ac}$  parallel to the plane of the magnetometer coils with a frequency  $\nu=100-150$  Hz. This parallel geometry means that there is no direct coupling between  $B_{ac}$  and the coils, as indicated in Fig. 2b. Since the coils are counter-wound, any misalignment with respect to  $B_{ac}$  will generate an equal and opposite voltage in each coil. However, if this parallel magnetic field magnetizes the sample, as indicated in Fig. 1b, then some of this secondary magnetic flux threads the two counter-wound coils in opposite senses, producing a voltage across the coils proportional to  $\partial M/\partial t$ . The complex susceptibility  $\chi$  was measured by phase sensitive detection of this voltage. The micro-magnetometers were designed to maximize the detection of this secondary flux, and those used in this work had either 80 or 120 turns per coil with a line width of  $\sim 2$  μm.

Two different superconducting samples were used in this study: a calibration sample of the ceramic high  $T_c$  cuprate YBCO; and a very high quality single crystal  $\alpha$ -uranium sample. Grains of YBCO were set in epoxy with the  $c$ -axes aligned by a magnetic field and machined into a half cylinder ( $r=0.5$  mm). Planar single crystals of  $\alpha$ -uranium were grown by electro-deposition in a salt bath at  $\sim 600$  °C with the  $c$ -axis perpendicular to the plane.<sup>14</sup> The residual resistivity ratio (RRR)  $\rho(300\text{ K})/\rho(2\text{ K})$  provides a measure of the sample's purity. Resistivity

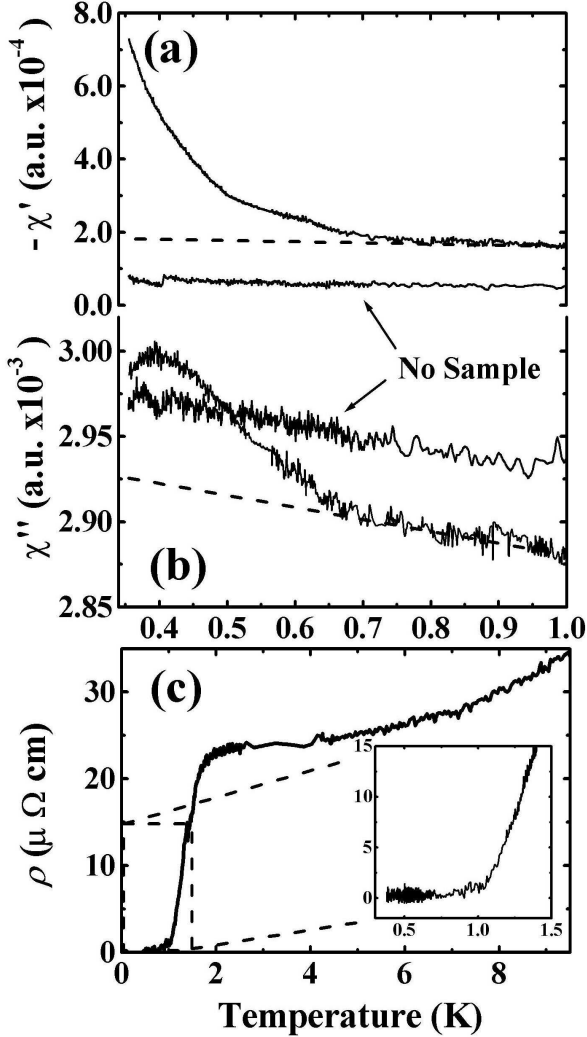


FIG. 3. Susceptibility vs. temperature for the single crystal  $\alpha$ -uranium sample. Both  $-\chi'$  (a) and  $\chi''$  (b) are shown with and without the  $\alpha$ -uranium sample present. Data were taken with  $|B_{ac}|=35$  mT and  $\nu=150$  Hz. Dashed lines indicate the slope of the “no sample” traces. (c) A plot of resistivity vs. temperature for the same sample. Data have been interpolated with minimal smoothing for clarity. The inset shows detail in the transition region.

measurements on this sample show a RRR of 206, three times larger than any previously reported, indicative of its high purity. Samples were mounted directly onto the magnetometers and the magnetometers attached to the CTls with epoxy. This assembly was inserted into a  $^3$ He cryostat giving access to  $T \geq 0.3$  K.

For a superconductor the real component of the susceptibility  $\chi'$  is a measure of the magnetic shielding and the imaginary component  $\chi''$  a measure of the magnetic irreversibility.<sup>19</sup> The signal which is in-phase with  $B_{ac}$  thus measures  $\chi'$  and the quadrature signal  $\chi''$ . In order

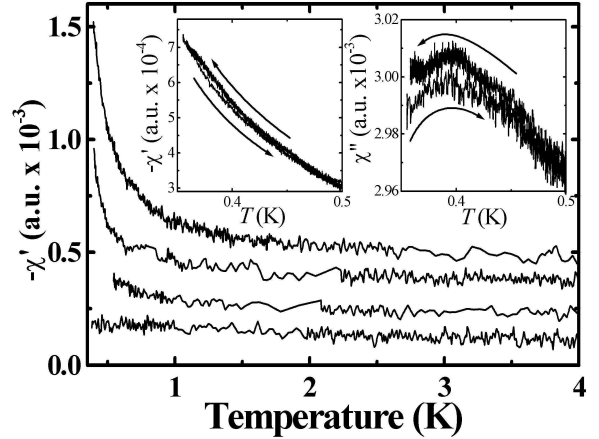


FIG. 4. Effect of dc magnetic field on magnetic susceptibility transition in single crystal  $\alpha$ -uranium. Plots of  $-\chi'$  with an applied static magnetic field  $B_{dc} = 0, 2.5, 3.8$  and  $12.5$  mT from top to bottom respectively. All data were obtained with  $|B_{ac}| = 35$  mT. Traces have been offset for clarity. The insets shows  $-\chi'$  and  $\chi''$  for increasing and decreasing  $T$ , indicated by arrows.

to verify the functionality of the micro-magnetometers, we first measured the YBCO calibration sample with  $B \parallel c$  (Fig. 2). In the normal state,  $T > T_c$ , YBCO is non-magnetic and there is no flux exclusion. Thus for  $T > 100$  K  $\chi'$  and  $\chi''$  are both close to zero. As the temperature is decreased below  $T_c$  ( $\sim 95$  K) supercurrents are set up to shield the interior of the sample from  $B_{ac}$ . This diamagnetic behavior leads to a negative  $\chi'$  which becomes more negative as  $T$  is reduced and more flux is expelled from the sample. In this mixed state the flux penetrating the sample lags the external flux resulting in the dissipation seen in the  $\chi''$  signal in Fig. 2. The peak in  $\chi''$  ( $\approx 95$  K) occurs when the flux is just penetrating as far as the center of the sample.<sup>19</sup> At lower  $T$  there is a flux free region at the center of the sample, which becomes larger as  $T$  is decreased further. The dissipation is now occurring in a smaller fraction of the sample volume and so  $\chi''$  now decreases. The inflection point in  $\chi'$  and maximum in  $\chi''$  are the characteristic signatures of a normal-superconducting transition.<sup>19</sup> Plots of  $\chi'$  near the inflection point for increasing and decreasing temperature sweeps show a small hysteresis (Fig. 2 inset), in agreement with established results. These results demonstrate the effectiveness of the micromagnetometers in reproducing known results using an established technique.

Figure 3 shows  $-\chi'$  and  $\chi''$  for a single crystal  $\alpha$ -uranium sample with an onset to superconductivity at  $T \approx 0.7$  K. The size of the features are much smaller here than for YBCO, however, corresponding “no sample” traces reveal that the structure is real and not due to

the measurement apparatus. In analogy with the YBCO data, we see a sharp rise in  $-\chi''$  ( $T \lesssim 0.7$  K) and a peak in  $\chi'$  ( $T \approx 0.4$  K). In the  $\alpha$ -uranium case the entire transition cannot be seen since it is not complete at the lowest temperature of the  $^3\text{He}$  system. However, the peak in  $\chi''$  at  $T \approx 0.4$  K is at the center of the transition, as for YBCO, and so the data in Fig. 3 represent more than half of the transition. Figure 3c shows the resistivity  $\rho$  as a function of  $T$  for the same sample. The data clearly show a superconducting transition with an onset at  $T \approx 1.8$  K and zero resistivity point at  $T \approx 0.8$  K. This confirms that the features in the susceptibility data are due to a normal-superconducting transition. The value of  $T_c$  for this sample ( $\sim 0.8$  K) is by far the highest reported for single crystal  $\alpha$ -uranium. This is in contrast to the accepted behavior which suggests that  $T_c$  decreases with increasing purity.<sup>1,23</sup>

If the transition in  $\chi$  is due to superconductivity, application of a dc magnetic field  $B_{dc}$  should move it to lower  $T$ . We confirm this by comparing plots of  $-\chi'(T)$  for  $B_{dc}=0, 2.5, 3.8$  and  $12.5$  mT in Fig. 4, which show that the superconducting behavior is rapidly quenched by a magnetic field. We note that although only a moderate field is required to suppress the superconductivity, our observation of a peak in  $\chi''(T)$  in Fig. 3 indicates that for  $T < 0.4$  K there is a flux free region in the sample. This confirms that the smaller features in  $-\chi'$  and  $\chi''$  for  $\alpha$ -uranium (Fig. 3) compared to YBCO (Fig. 2) are not due to penetration of a too large  $B_{ac}$  through the whole sample. Measurements for increasing and decreasing  $T$  near the transition reveal that hysteresis effects in  $-\chi'$  and  $\chi''$  are close the noise limit (Fig. 4 insets). We have also examined the frequency dependence of this transition and find no measurable effect over the range  $\nu=100\text{-}150$  Hz (not shown).

While there has been some controversy surrounding claims of bulk superconductivity based on susceptibility, it is widely accepted that these measurements can be used to estimate the superconducting volume fraction.<sup>19</sup> If the YBCO and  $\alpha$ -uranium samples had identical geometries, a direct comparison of flux exclusion could be made by comparing the size of the transition features in  $\chi'$ , using the arbitrary units which are the same in Figs. 2 and 3. Given that the sample dimensions are comparable and YBCO is a bulk superconductor, we estimate that the  $\alpha$ -uranium excludes a flux equivalent to  $\sim 1\%$  of the sample volume. While this is a fairly crude estimate, the difference in transition heights for the two samples is more than two orders of magnitude, and so clearly significant.<sup>24</sup> The London penetration depth  $\lambda_L$  can affect the inferred superconducting fraction,<sup>19</sup> but it cannot account for the much smaller transition observed here.

The conclusion that superconductivity in  $\alpha$ -uranium is filamentary was dispelled by heat capacity measurements which revealed bulk superconductivity in *polycrystalline* samples.<sup>12</sup> However, the results presented here on *single crystal* samples suggest that the superconducting

state is filamentary, based on the volume fraction arguments above. The polycrystalline result<sup>12</sup> may in fact be due to strain at grain boundaries ( $\alpha$ -uranium has highly anisotropic coefficients of thermal expansion<sup>1</sup>), giving rise to a similar bulk effect as induced at high  $P$ .<sup>10,11</sup> Impurity effects have been proposed as a mechanism for filaments in  $\alpha$ -uranium,<sup>1,10</sup> but these should be negligible in our high-purity sample. Strain arising from the anisotropic thermal expansion has also been suggested,<sup>1,9</sup> however this should not be relevant in these single crystals.<sup>13</sup> Indeed, a Debeye temperature  $\theta_D=256$  K, close to the value of 250 K obtained from elastic constant measurements suggests that the lattice is strain free, in contrast to polycrystalline samples.<sup>13</sup> A more exotic explanation is that the distortions in the crystal lattice due to the CDW state are somehow responsible for causing superconducting filaments. Resistivity measurements on these samples show clear signatures of the CDW transitions at 43, 37, and 22 K.<sup>13,25,26</sup>

The coplanar micro-magnetometers described here are compatible with the extreme environment of  $\mu\text{s}$  pulsed magnetic fields, required for future low  $T$  de Haas-van Alphen measurements of  $\alpha$ -uranium and high- $T_c$  superconductors such as YBCO. We have previously demonstrated the capability to make electrical transport measurements in ms pulsed fields  $> 50$  T<sup>27</sup> and  $\mu\text{s}$  pulsed fields  $> 100$  T using the CTL and sample mounting technology used here.<sup>15–18</sup> The CTLs were specifically designed to eliminate  $dB/dt$  pickup and the absence of connecting wires to the magnetometers makes this system ideally suited to such an environment. Previous de Haas-van Alphen measurements on  $\text{LaB}_6$  and  $\text{CeB}_6$  in ms pulsed magnetic fields  $> 50$  T (Ref. 28) support this, while the present work demonstrates extremely sensitive measurements using these coplanar micro-magnetometers.

In summary, these results represent the first measurements of the complex magnetic susceptibility of a superconducting transition in high-purity single crystal  $\alpha$ -uranium. They suggest that  $T_c$  increases with purity, and indicate that the superconducting state may be filamentary. This has not been reconciled with recent results<sup>13</sup> and further calorimetric measurements to lower  $T$  are required to resolve this issue. Two outstanding questions in the  $\alpha$ -uranium picture of particular interest are how superconductivity and the CDW states coexist, and a complete understanding of the CDW state itself. The high purity single crystal samples and coplanar micro-magnetometers reported here offer a promising route to answering these questions. This will require a mapping of the Fermi surface to determine why particular values of the wavevector are favourable for the formation of a CDW state.<sup>1</sup>

We would like to thank J. C. Lashley and K. -H. Müller for useful discussions. This work was supported by the Australian Research Council. Work at Los Alamos was performed under the auspices of the US Dept. of Energy. The National High Magnetic Field Laboratory is

\* electronic mail: job@physics.uq.edu.au.

<sup>1</sup> G. H. Lander, E. S. Fisher, and S. D. Bader, *Adv. Phys.* **43**, (1994) and Refs. therin.

<sup>2</sup> R. D. Fowler *et al.*, *Phys. Rev. Lett.* **15**, 860 (1967).

<sup>3</sup> H. G. Smith, N. Wakabayashi, W. P. Crummett, and R. M. Nicklow, *Phys. Rev. Lett.* **44**, 1612 (1980).

<sup>4</sup> L. Fast *et al.*, *Phys. Rev. Lett.* **81**, 2978 (1998).

<sup>5</sup> A. Hjelm, O. Eriksson, and B. Johansson, *Phys. Rev. Lett.* **71**, 1459 (1993).

<sup>6</sup> E. S. Fisher, *J. Alloys Compounds* **213/214**, 254 (1994) and Refs. therin.

<sup>7</sup> J. E. Gordon *et al.*, *Phys. Rev.* **152**, 432 (1966).

<sup>8</sup> J. C. Ho, N. E. Phillips, and T. F. Smith, *Phys. Rev. Lett.* **17**, 694 (1966).

<sup>9</sup> T. H. Geballe *et al.*, *Science* **152**, 755 (1966).

<sup>10</sup> W. E. Gardner and T. F. Smith, *Phys. Rev.* **154**, 309 (1967).

<sup>11</sup> T. F. Smith and W. E. Gardner, *Phys. Rev.* **140**, 1620 (1965).

<sup>12</sup> S. D. Bader, N. E. Phillips, and E. S. Fisher, *Phys. Rev. B* **12**, 4929 (1975).

<sup>13</sup> J. C. Lashley *et al.*, *Phys. Rev. B* **63**, 224510 (2001).

<sup>14</sup> C. C. McPheeers, E. C. Gay, P. J. Karel, and J. P. Ackerman, *JOM* **49**, n7 22 (1997).

<sup>15</sup> B. E. Kane *et al.*, *Rev. Sci. Instrum.* **68**, 3843 (1997).

<sup>16</sup> A. S. Dzurak *et al.*, *Phys. Rev. B* **57**, 14084 (1998).

<sup>17</sup> J. L. O'Brien *et al.*, *Phys. Rev. B* **61**, 1584 (2000).

<sup>18</sup> J. S. Brooks *et al.*, in *Proceedings of the Eighth International Conference on Megagauss Magnetic Field Generation and Related Topics, Tallahassee, 1998*, edited by H. Schneider-Muntau (World Scientific, Singapore).

<sup>19</sup> F. Gömöry, *Supercond. Sci. Technol.* **10**, (1997), and references therin.

<sup>20</sup> M. B. Ketchen and J. M. Jaycox, *Appl. Phys. Lett.* **40**, 736 (1982).

<sup>21</sup> J. G. E. Harris *et al.*, *Appl. Phys. Lett.* **75**, 1140 (1999).

<sup>22</sup> M. J. Naughton *et al.*, *Rev. Sci. Instrum.* **68**, 4061 (1997).

<sup>23</sup> A strong dependence on sample purity was a clue to the pairing mechanism in  $\text{Sr}_2\text{RuO}_4$  [A. P. Mckenzie *et al.*, *Phys. Rev. Lett.* **80**, 161 (1998)] and in  $\text{UPt}_3$  [Y. Dalichaouch *et al.*, *Phys. Rev. Lett.* **75**, 3938 (1995)].

<sup>24</sup> The broad nature of this transition might be related to the details of the superconducting filaments.

<sup>25</sup> J. L. Smith *et al.*, *J. Supercon.: Incorp. Nov. Mag.* **13**, 833 (2000).

<sup>26</sup> J. L. Smith *et al.*, (2001). to appear

<sup>27</sup> J. S. Brooks *et al.*, *Phys. Rev. B* **59**, 2604 (1999).

<sup>28</sup> R. G. Clark *et al.*, (1998), proc., 8th Intl. Conf. on Megagauss Magnetic Field Generation and Related Topics, Oct. 1998, Tallahassee, USA.